Journal of Huntington's Disease 1 (2012) 243–260
DOI 10.3233/JHD-120038
IOS Press



Research Report

# Caspase-6-Resistant Mutant Huntingtin Does not Rescue the Toxic Effects of Caspase-Cleavable Mutant Huntingtin *in vivo*

Rona K. Graham[a], Yu Deng[b], Mahmoud A. Pouladi[c,d], Kuljeet Vaid[b], Dagmar Ehrnhoefer[b], Amber L. Southwell[b], Nagat Bissada[b], Sonia Franciosi[b] and Michael R. Hayden[b,*]
[a]*Research Center on Aging, Department of Physiology and Biophysics, University of Sherbrooke, Sherbrooke, QC, Canada*
[b]*Centre for Molecular Medicine and Therapeutics, Child and Family Research Institute, Department of Medical Genetics, University of British Columbia, Vancouver, BC, Canada*
[c]*Translational Laboratory in Genetic Medicine, Agency for Science, Technology and Research, Singapore, Republic of Singapore*
[d]*Department of Medicine, National University of Singapore, Singapore, Republic of Singapore*

**Abstract**.
**Background:** The amelioration of behavioral and neuropathological deficits in mice expressing caspase-6-resistant (C6R) mutant huntingtin (mhtt), despite the presence of an expanded polyglutamine tract, highlights proteolysis of htt at the 586aa caspase-6 (casp6) site may be an important mechanism in the pathogenesis of Huntington disease (HD). One possible explanation of these effects is that C6R mhtt could act as a dominant negative on mhtt.
**Objective and Methods:** To determine if the neuroprotective effect observed in the C6R mice is due to dominant negative effects, we crossed the C6R mice to the YAC128 HD mouse model to generate mice expressing both caspase-cleavable and C6R mhtt (YAC/C6R) concurrently and assessed previously defined behavioral and neuropathological endpoints.
**Results:** Our results demonstrate that YAC/C6R animals exhibit similar motor abnormalities and learning deficits as the YAC128 mice. Neuropathological analysis reveals a significant decrease in brain weight and striatal volume in the YAC/C6R mice comparable to the YAC128 mice. In contrast, and similar to previous findings, C6R mice demonstrate preserved brain weight and striatal volume. As expected, body weight is significantly increased in the YAC/C6R mice due to the increased levels of htt.
**Conclusions:** The results of this study suggest that the lack of an HD phenotype in the C6R mice is most likely due to the absence of cleavage of htt and not due to suppression of expression of mhtt.

Keywords: Huntington disease, mutant huntingtin, caspase-6, apoptosis, human, mouse models

## INTRODUCTION

Huntington disease (HD), caused by an expanded CAG repeat in the gene encoding huntingtin (htt), is a fatal neurodegenerative disease characterized by progressive deterioration of cognitive and motor function [1]. There is strong evidence that apoptosis plays a role in the neurodegeneration observed in HD [2–5]. Apoptosis is a genetically programmed form of cell death that utilizes caspases, a family of cysteine proteases that are activated by proteolytic processing and dimerization. Increased DNA fragmentation

*Correspondence to: Michael R. Hayden, Centre for Molecular Medicine and Therapeutics, University of British Columbia, 980 West 28th Avenue, Vancouver, BC V5Z 4H4, Canada. Tel.: +1 604 875 3535; Fax: +1 604 875 3819; E-mail: mrh@cmmt.ubc.ca.

ISSN 1879-6397/12/$27.50 

and typical apoptotic, TUNEL positive cells have been detected in human HD brain [4, 6]. Furthermore, activation of caspases is observed in human and murine HD brain and the pro-apoptotic protein Bax is increased compared to controls [2–4]. Indeed, htt was the first neuronal caspase substrate identified [7]. Proteolytic cleavage of htt by caspases releases an amino terminal fragment containing the glutamine tract [7–11]. Expression of htt fragments containing an expanded polyglutamine repeat are toxic *in vitro* and *in vivo* [12, 13], and accumulation of N-terminal truncated products of htt are observed in postmortem brain tissue from HD subjects, as well as in mouse models of HD [9, 10, 14].

Numerous caspase substrates have active roles in apoptosis, in particular as a result of the fragments generated. The stress-induced generation of caspase-cleaved proteolytic fragments has been shown to trigger toxicity and amplify the cell death response in several experimental paradigms [15–23]. For example, caspase-dependent cleavage of CDC25A generates an active fragment that activates cyclin-dependent kinase 2 during apoptosis [16] and casp6-cleavage of NF-κß generates a pro-apoptotic fragment which induces cell death [15] and disrupts the pro-survival signaling pathway. In HD, the 586aa htt fragment is observed in affected brain regions and importantly, murine models expressing the 586aa mhtt fragment develop neurological abnormalities similar to those observed in other HD mouse models [9, 24–27]. In AD brain tissue, p97, a valosin containing ubiquitin dependent ATPase, is cleaved by casp6 and the resultant fragment impairs the proteasome and destabilizes endogenous p97 [18]. Of interest, casp6 cleaved tau is observed in AD and HD brain, and levels of casp6 cleaved tau in human brain inversely correlate with global cognitive scores [2, 28, 29].

Similar to htt, APP is also cleaved by caspases during apoptosis [30–32]. Two casp6 cleavage sites within APP (at residues 653 and 664) have been identified *in vitro* [31, 32]. Cleavage of APP at the 664aa site has been detected in early-stages of disease in human AD brain tissue [33, 34] and is a necessary requirement for nuclear p21-activated kinase signalling [35], and deficits in synaptic transmission and learning in AD mouse models [36].

Additional evidence supporting the role of caspase-generated fragments in the pathogenesis of neurodegenerative diseases derives from studies on the caspase resistant form of a caspase substrate. Expression of a mutation that eliminates cleavage at the 586aa site of mutant htt [i.e. Casp6- resistance (C6R) mhtt] is sufficient to preserve striatal volume and cognitive and motor function in a yeast artificial chromosome (YAC) model of HD [2, 9, 37, 38], as well as preventing alterations in extrasynaptic NMDA receptor activation [39]. These results are compatible with proteolysis of htt at the 586aa cleavage site being a important step in the pathogenesis of HD. Furthermore, in contrast to the active casp6 observed in the brains of pre-symptomatic and early-grade human HD patients as well as murine HD models, *in vivo* expression of C6R mhtt attenuates casp6 activation [2].

Inhibiting cleavage of APP at residue 664 also provides partial rescue from behavioural deficits and neuropathology in an AD mouse model [34–36, 40–42], providing proof-of-principle for the importance of cleavage at this particular site within APP in the pathogenesis of AD. Furthermore, activation of casp6 and cleavage of a number of casp6 substrates is observed in early-stage AD human brain [18, 28–30, 43, 44].

In general, inhibiting the cleavage of a caspase substrate has been shown to confer protection in numerous experimental paradigms [2, 9, 11, 15, 20, 37–39, 45–56]. An unresolved question is whether the neuroprotection observed upon expression of a caspase-resistant substrate, such as C6R mhtt, is due to dominant-negative effects such as suppression of mhtt expression and/or casp6 activation. Prior to assessing this, it is important to rule out other factors that may influence the phenotype or lack thereof in the C6R mice. Studies in HD patients and mouse models reveal a clear relationship between levels of mhtt and the severity of the HD phenotype. If mhtt transgene expression levels and/or CAG size were decreased in the C6R mice compared to the YAC128 lines this may suggest they are protected as they would present with a less severe phenotype. The C6R mice have 13CAGs more than the YAC128 line [9], thus, the C6R lines do have a CAG size that is at least as large as the control YAC128 lines. Furthermore we have previously shown that transgene levels in the C6R mice are most comparable to YAC128 line HD53 [9]. We have extended that analysis here and include copy number and validation of RNA and protein transgene expression levels in a new cohort of YAC mice.

If the neuroprotection observed in C6R mice reflects a dominant-negative effect such as suppression of mhtt expression then similar protection and amelioration of HD-related phenotypes may be expected in mice expressing both caspase-cleavable and C6R mhtt. In order to address this question we crossed the YAC128 mice to the C6R mice to generate mice expressing both caspase-cleavable and C6R mhtt (YAC/C6R)

and assessed previously defined behavioral and neuropathological endpoints.

## MATERIAL AND METHODS

### *HD transgenic mice*

YAC128 and C6R (lines C6R7 and C6R13) mice were generated as described [9, 57]. All murine tissues harvested according to UBC Animal Protocol A07-0106.

### *Real-time quantitative PCR to determine HTT transgene DNA level*

Mouse genomic DNA was extracted from tail samples and 0.08 ng of the genomic DNA used in a final volume of 10 ul with Power SYBR Green PCR Master Mix (ABI). Human-specific huntingtin primers and mouse-specific beta-actin primers as described [58] were used at the final concentration of 100 nM. Comparative Ct Assay was performed using ABI 7500 Fast Real-Time PCR System under default condition. The relative transgene DNA levels were normalized to mouse β-actin.

### *Real-time quantitative RT-PCR to determine transgenic mRNA expression level*

Total RNA was extracted from mouse cortex with RNeasy Mini Kit or RNeasy Micro Kit (Qiagen) and treated with Amplification Grade DNaseI (Invitrogen). First-strand cDNA was prepared from 1 μg of total RNA using SuperScriptIII First-Strand Synthesis System (Invitrogen). cDNA from 2 ng of total RNA was used in a final volume of 10 μl with Power SYBR Green PCR Master Mix (ABI). Comparative Ct Assay was performed using ABI 7500 Fast Real-Time PCR System under default condition. All samples were run in triplicate. mRNA expression levels of target genes were normalized to β-actin. Human specific HD and mouse β-actin primers were as described [58].

### *Protein analysis and western blotting*

Murine tissue protein lysates were prepared as described previously [2]. Immunoblots for huntingtin were probed using MAB1574 (1 : 2000, Chemicon) or MAB2166 (1 : 2000, Chemicon)and Calnexin (1 : 10,000, Sigma) antibodies. All immunoblotswere prepared following standard procedures and used infrared-labeled secondary antibodies, Immobilon-PVDF-FL membranes and the Li-Cor Odyssey Infrared imaging system (BioSciences). Quantitative analysis of immunoblotting was based on the integrated intensity from Li-Cor Odyssey software (v2.0). Calnexin was used as loading control.

### *FRET assay for the quantification of soluble mHtt*

Detection of mutant htt in plasma samples was performed as described previously [59]. Monoclonal BKP1 antibody raised against the htt N-terminus [60] and monoclonal MW1 antibody raised against the expanded polyglutamine tract of mHtt were labelled with terbium or D2 (Cisbio Bioassays) fluorescent tags, respectively. Antibodies were mixed in 50 mM $NaH_2PO_4$, 0.1% bovine serum albumin (BSA), and 0.05% Tween 20 at 1 ng/μl BKP1-terbium and 10 ng/μl MW1-D2. To each 20 μl plasma sample, 2 μl of antibody master mix was added in a white 384 well plate, and plates were measured with a xenon lamp Victor Plate Reader (Perkin Elmer) after excitation at 340 nm (time delay 50 ms, window 200 ms). The signal measured at 615 nm resulted from the emission of the terbium-labeled antibody and was used for normalization of potential signal artefacts. The htt-specific signal at 665 nm resulted from emission of the D2-labeled antibody after time-delayed excitation by the terbium. The relative mhtt concentration is represented by the 665/615-nm ratio.

### *Rotarod*

Motor coordination and learning were assessed by accelerating rotarod (UGO Basile) testing. Two month old mice were trained for 3 consecutive days during 3, 120 s trials per day with a 2 hour inter-trial interval. Mice falling from the rod were returned, to a maximum of 10 falls/trial. The time to first fall and number of falls per trial were recorded, and the average of the three trials was scored. For longitudinal rotarod assessment, 2 and 4 month old mice were tested on a rod accelerating from 5 to 40 RPM over 300 seconds. Latency to the first fall was recorded and the average of 3 trials was scored.

### *Novel object location*

To assess spatial learning by preference for a known object in a novel location, 4 month old mice were placed in the lower left corner of a 50 × 50 cm open grey acrylic box with 20 cm sides and allowed to acclimate for 5 minutes. Mice were then removed from the

box for a 5 min ITI and two different novel objects are placed in the upper two corners of the box, far enough from the sides so as to not impede movement around the outer edge (7 cm). Mice were reintroduced to the box in the lower left corner and recorded for 5 min by a ceiling mounted video camera, during which the frequency and duration of investigations of the objects was scored by Ethovisionxt 7.0 animal tracking software. Mice were then removed from the box for a 5 min ITI, and the object at the top right corner of the box was moved to the lower right corner of the box. Mice were then reintroduced to the box and recorded for 5 min during which the frequency and duration of investigations of the objects was scored. The percentage of the investigations to the object in the new location was computed.

*Neuropathology*

All quantitative analysis was done blind with respect to genotype as described previously [9, 57]. Briefly, mice were weighed then terminally anesthetized by intraperitoneal injection of 2.5% avertin and perfused with 3% paraformaldehyde/0.15% glutaraldehyde in PBS. The brains were stored in 3% paraformaldehyde for 24 h at 4°C then removed and stored in PBS + Azide. Mouse brains were weighed and then cut using a vibratome and coronal sections (25 μm) spaced 200 μm a part through out the striatum were stained with Neu N antibody (Chemicon, Teme- cula, CA) at 1 : 1000 dilution. Biotinylated secondary antibodies (Vector) were used at 1 : 1000 prior to signal amplification withan ABC Elite kit (Vector) and detection with DAB (Pierce, Rock- ford, IL).

The perimeter of the striatum for each section was traced using Stereo Investigator 10 software (Microbrightfield, Williston, VT, USA). Striatal volume was determined using the Cavalieri principle where the area of each striatum per section was summed and multipled by the section thickness (25 microns) and section sampling interval (every eighth section) as previously described [61].

*Immunohistochemistry*

Mouse brains were fixed and sectioned as described above then immunoassayed with DARPP-32. Quantification of DARRP-32 was performed on 25 μm free-floating sections from WT, YAC128, C6R and YAC/C6R mice. The primary antibody used was mouse anti-DARPP32, #C24-6a (gift from Dr. Paul Greengard and Dr. HughHemming; 1 : 20,000). Sections incubated without primary antibody served as controls. Sections were washed and incubated with horseradish peroxidase (HRP) conjugated secondary antibody (1 : 500, Jackson ImmunoResearch Laboratories). Staining was visualized using DAB and counter stained with 0.5% cresyl violet. Sections were photographed using a Zeiss Axioplan 2 microscope and Cool snap HQ Digital CCD camera (Photometrics). The amount of DARPP32 was determined using Meta Morph software version 6.3 (Universal Imaging Corporation). Labeling was identified using constant threshold levels for all images and analyzed using "integrated morphometry. Relative levels of staining were calculated as the sum of the integrated optical density (IOD) for each image divided by the area of the region selected then multiplied by the sampling interval (8) and section thickness (25 μm). No staining was observed in a negative control without primary antibody.

*Assessment of nuclear huntingtin and inclusions*

WT, YAC128, C6R and YAC/C6R lines were immunoassayed with the polyclonal antibody EM48 to assess for the presence of nuclear htt and inclusions as described previously [9] using EM48 at 1 : 2000 and DAB as the chromogen (Vector). Htt inclusions were defined as EM48 positive punct a visible at the light microscope levels. Photographs were taken on a light microscope (Zeiss) using 100 objective. The number of cells containing huntingtin inclusions were quantified from EM48 stained sections using stereological techniques. Briefly, every 24th section spanning from Bregma 1.42 mm to −0.82 mm with a total of four sections per mouse were utilized in the analysis. Striatum and cortex in each section were delineated at low magnification (2.5×). Cells that were considered positive for htt inclusions were designated as cells containing intense, darkly stained particulates. Total positively stained cells were estimated using a 40× objective and the Fractionator Probe with a counting frame of 25 × 25 and grid size of 250 × 250 for striatum and 500 × 500 for cortex of the stereology software (StereoInvestigator 10; MBF Bioscience; Williston, VT). Analysis was performed with the investigator blind to genotype.

*Statistical analysis*

Statistical analysis was done using Student's *t*-test, one-way and two-way ANOVA (in cases of significant effect of genotype, *post-hoc* comparisons between genotypes were performed using Bonferroni).

$p$ values, SEM, means and standard deviations were calculated using Graphpad Prism version 5.0. Differences between means were considered statistically significant if $p < 0.05$.

## RESULTS

### *Transgene levels in YAC mice*

As the phenotype of HD is significantly influenced by levels of expression of mhtt [58, 62–66], it is essential to control for this parameter in order to determine if C6R mhtt can rescue the toxic effects of caspase-cleavable mhtt *in vivo*. We therefore first re-assessed which YAC128 line has transgene expression levels most similar to the C6R mice. In order to match transgene expression in C6R murine brain tissue to the most appropriate YAC128 line we assessed copy number, mRNA and protein transgene levels in the C6R (C6R7 and C6R13) and YAC128 (HD54, HD55 and HD53) lines of mice ($n = 3$, age-matched). A comparison of HD gene copy number in the YAC128 and C6R lines demonstrates that transgene copy number in the C6R mice is most similar to the previously described YAC128-HD53 mice (ANOVA $p = 0.0001$, Fig. 1A). Assessment of mhtt mRNA levels demonstrates that cortical transgene mRNA expression in the C6R mice are most similar to the YAC128-HD53 mice and higher than YAC128-HD55 as found previously [9, 67] (ANOVA $p = 0.0001$; YAC128-HD53 vs. C6R7 $p > 0.05$; YAC128-HD55 vs. C6R7 $p < 0.001$; YAC128-HD54 vs. C6R7 $p < 0.001$; Fig. 1B). Immunoblotting with several different htt antibodies reveals that full-length mhtt levels in C6R cortex are intermediate between HD53 and HD55 transgene levels (Fig. 1C–D). However, as proteolysis of htt in the C6R and YAC128 brain tissue will affect full-length mhtt levels this may not provide an accurate estimation of true levels of total mhtt. This causes difficulties in determining total transgene protein levels in these mice. We therefore assessed soluble htt levels in plasma where protease activation may be expected to be at a minimum. Using this method demonstrates that mhtt levels in C6R vs YAC128-HD53 are not significantly different (Fig. 1E, $n = 12$, $p = 0.68$). However, YAC128-HD53 and HD55 do show a significant difference in soluble htt levels (Fig. 1E, $n = 12$, $p = 0.03$) and there is a trend towards a decrease in soluble mhtt levels in HD55 compared to C6R ($p = 0.06$). We also assessed body weight in the YAC128 and C6R lines as levels of mhtt have been shown to influence this parameter [68, 69]. Analysis of body weight at 12 months of age in the various lines demonstrates that the C6R mice are most closely matched to YAC128-HD53 line ($n = 15$, female, ANOVA $p = 0.001$; C6R vs. HD53 $p > 0.05$; C6R vs. HD55 $p < 0.01$; HD53 vs. HD55 $p < 0.01$; Fig. 1F). The C6R7 mice were chosen, based on the general analysis, for further investigation to cross to the mutant htt line. Similarly, based on the above results, the YAC128-HD53 line was chosen as the YAC128 line for the cross.

### *Generation and characterization of YAC/C6R mice*

Using breeding strategies with YAC128-HD53 and C6R7 mice, we developed a YAC/C6R line. Mhtt mRNA levels in the cortex of YAC/C6R mice are higher than either YAC128 or C6R cortical tissue as expected ($n = 3$, ANOVA $p = 0.015$; YAC/C6R vs. YAC128 $p < 0.05$; YAC/C6R vs. C6R $p < 0.05$; Fig. 2A). Assessment of full-length mhtt protein levels demonstrates that YAC/C6R cortex contains ∼25% (using 1C2 htt antibody, $n = 3$, Fig. 2B) or ∼49% (using MAB2166 htt antibody, $n = 3$, Fig. 2C, trend towards increased htt in YAC/C6R, ANOVA $p = 0.09$) increase in levels of mhtt vs. YAC128 mice. We also determined htt levels in the plasma of the cross mice. Our results demonstrate that mhtt levels in the plasma of YAC/C6R mice are significantly higher than YAC128 (42% increase) or C6R (41% increase) mhtt plasma levels ($n = 14$, ANOVA $p = 0.0008$, YAC128 vs. YAC/C6R $p < 0.01$; C6R vs. YAC/C6R $p < 0.05$, Fig. 2D). Evaluation of body weight in all genotypes from the cross (WT, YAC128, C6R and YAC/C6R) reveals that female body weights in the transgenic mice at 3 and 12 month of age demonstrate a significant increase compared to WT (3 months: ANOVA $p = 0.0001$, Fig. 3A; 12 months: ANOVA $p = 0.0001$, Fig. 3B). No difference in male body weights were observed at 3 months of age in the transgenic YAC vs. WT mice (Fig. 3C). However, at 12 months of age, male body weights in the YAC mice are significantly higher than WT (ANOVA $p = 0.0001$, Fig. 3D).

### *Motor abnormalities and spatial learning deficits in YAC/C6R mice*

As previously shown, YAC128 mice demonstrate motor abnormalities, depression and cognitive deficits including difficulties in changing strategies, delayed platform finding and impaired spatial learning [37, 57, 70–72]. To determine if YAC/C6R mice demonstrate

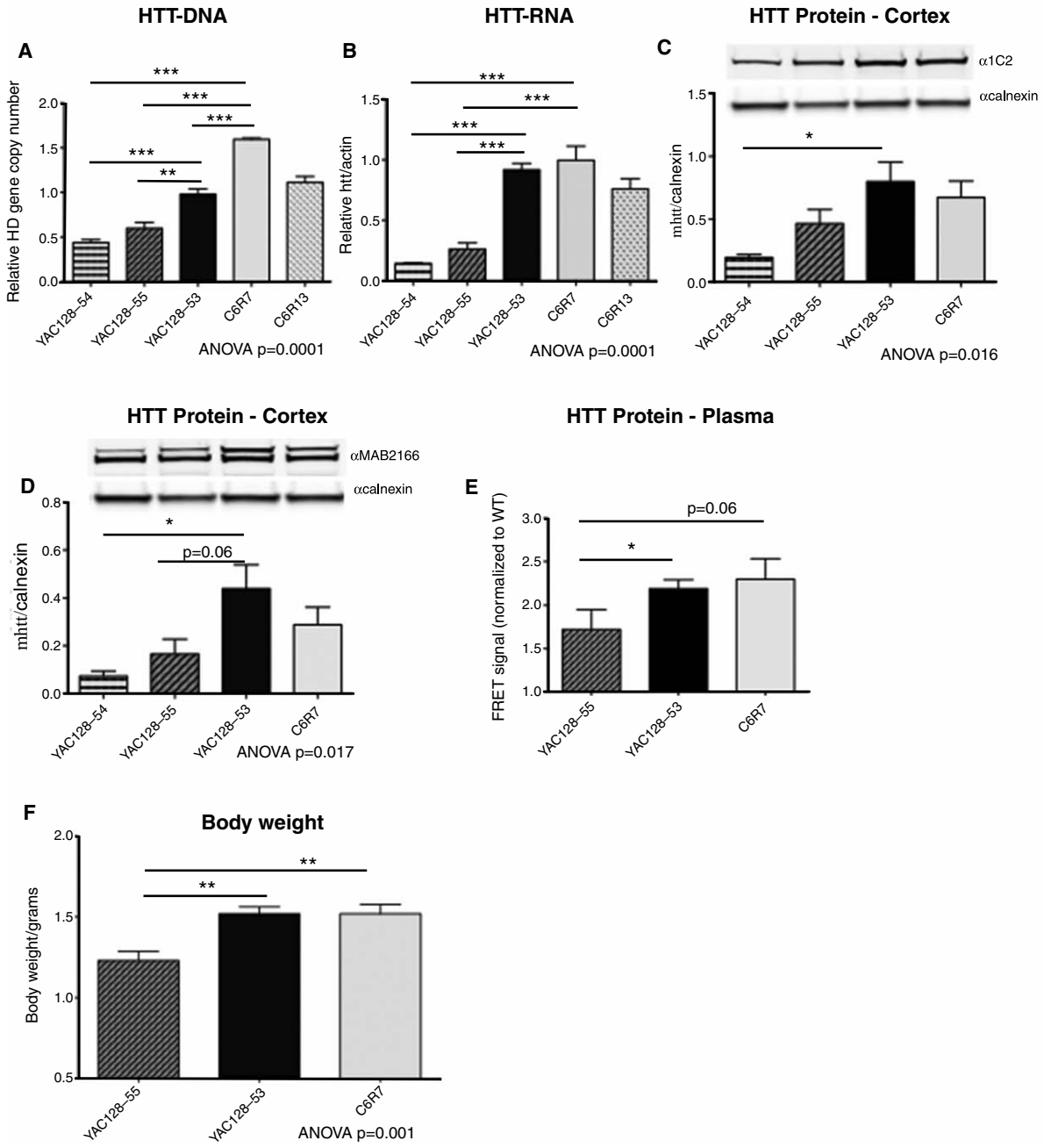


Fig. 1. Transgene levels in YAC mouse models. A) HD gene copy number in YAC128 and C6R lines demonstrates copy number in the C6R mice is most similar to YAC128-HD53 mice ($n=3$, ANOVA $p=0.0001$). B) Cortical transgene mRNA expression in the C6R mice are most similar to the YAC128-HD53 mice and higher than YAC128-HD55 ($n=3$, ANOVA $p=0.0001$; YAC128-HD53 vs. C6R7 $p>0.05$; YAC128-HD55 vs. C6R7 $p<0.001$; YAC128-HD54 vs. C6R7 $p<0.001$). Westerns blots probed with C) 1C2 or D) MAB2166 antibodies demonstrates that full-length mhtt levels in C6R cortex are intermediate between HD53 and HD55 transgene levels (1C2: $n=4$, ANOVA $p=0.016$, HD53 vs. C6R $p>0.05$; HD53 vs. HD54, $p<0.05$; MAB2166: $n=4$, ANOVA $p=0.017$, HD53 vs. C6R, $p>0.05$; HD53 vs. HD54, $p<0.05$). E) Soluble htt levels in plasma demonstrate that mhtt levels in C6R vs. YAC128-HD53 are not significantly different ($n=12$, $p=0.68$). However, YAC128-HD53 vs. HD55 show a significant difference in soluble htt levels ($n=12$, $p=0.03$) and a trend towards a decrease in soluble mhtt levels in HD55 vs. C6R ($p=0.06$). F) Analysis of body weight at 12 months of age demonstrates that the C6R mice are most closely matched to YAC128-HD53 line ($n=15$, female, ANOVA $p=0.001$; C6R vs. HD53 $p>0.05$; C6R vs. HD55 $p<0.01$; HD53 vs. HD55 $p<0.01$). *$p<0.05$; **$p<0.01$; ***$p<0.001$.

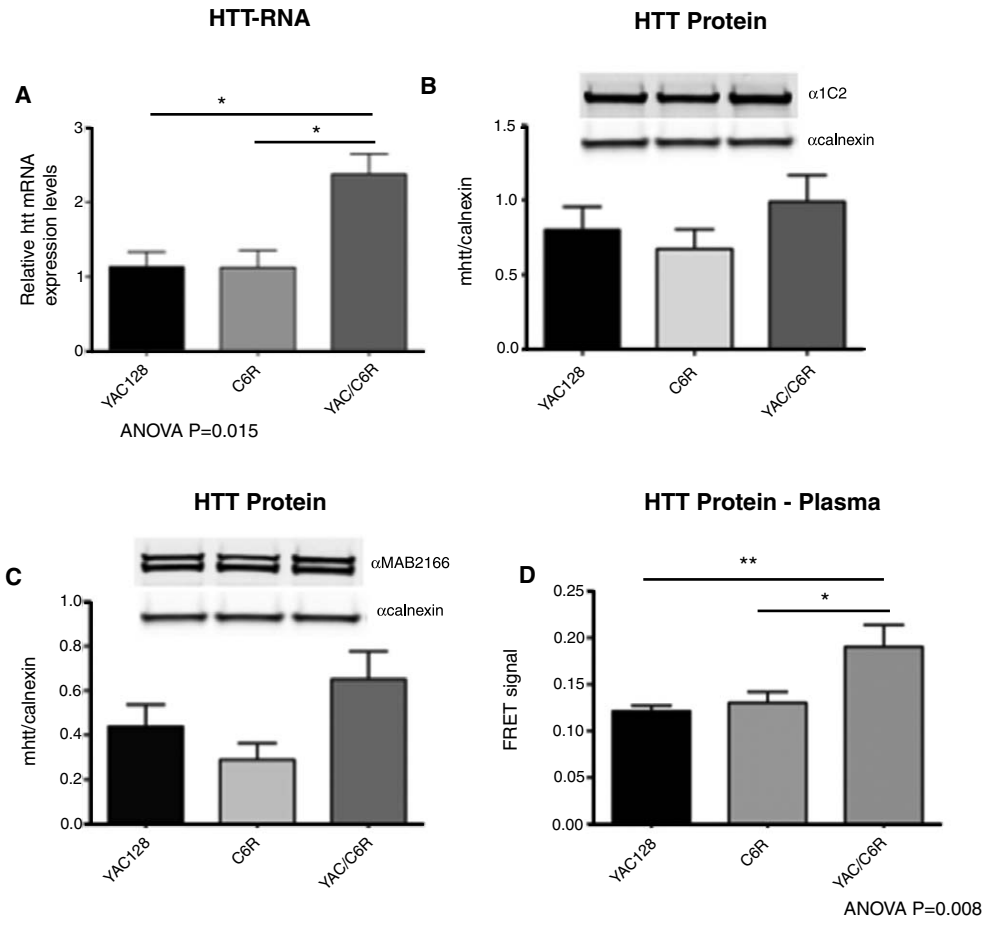


Fig. 2. Transgene levels in YAC/C6R mice. The double mutant line (YAC/C6R) is the result of a breeding of YAC128-53 and C6R7 mice. A) Mhtt mRNA levels in the cortex of YAC/C6R mice are higher than either YAC128 or C6R cortical tissue ($n = 3$, ANOVA $p = 0.015$; YAC/C6R vs.YAC128 $p < 0.05$; YAC/C6R vs. C6R $p < 0.05$). B) Assessment of full-length mhtt protein levels demonstrates that YAC/C6R cortex contains ~25% (1C2 htt antibody, $n = 3$) or C) ~49% (MAB2166 htt antibody, $n = 3$) increase in levels of mhtt vs. YAC128 mice. D) Mhtt levels in the plasma of YAC/C6R mice are significantly higher than YAC128 (42% increase) or C6R (41% increase) mhtt plasma levels ($n = 14$, ANOVA $p = 0.0008$, YAC128 vs. YAC/C6R $p < 0.01$; C6R vs. YAC/C6R $p < 0.05$). *$p < 0.05$; **$p < 0.01$.

behavioral deficits we assessed rotarod performance and preference for a novel object in WT, YAC128, YAC/C6R and C6R cohort of mice. At 2 and 4 months of age rotarod deficits are observed in mice expressing YAC/C6R mhtt (2 months ANOVA $p = 0.009$, WT vs. YAC/C6R $p < 0.01$, C6R vs. YAC/C6R $p < 0.05$, Fig. 4A; 4 months ANOVA $p < 0.019$, WT vs. YAC/C6R $p < 0.05$, Fig. 4B; body weight of behavior tested mice Fig. 4D–G). To assess spatial learning by preference for a known object in a novel location, 4 month old mice were habituated to an open field for 5 minutes. Mice were then removed from the box for a 5 min inter-trial interval (ITI) and then exposed to two novel objects in the open field (T1). Investigations of the novel objects were scored. Mice were then removed from the box for a 5 min ITI, and the object at the top right corner of the box was moved to the lower right corner of the box. The mice were then reintroduced to the box. Investigation of each object was scored for 5 min and the percentage of the investigations to the target object, the one in the novel location, determined (T2). A score of 50% indicates no preference. WT and C6R mice display a preference for the novel object location (two-way ANOVA, genotype $p = 0.04$; $F = 2.73$, Bonferroni *post hoc* C6R trial 1 vs. trial 2 $p < 0.05$; WT not significant by *post hoc* but are by *t*-test $p = 0.017$, Fig. 4C). However, YAC128 and YAC/C6R mice display no preference in either trial indicating impaired spatial learning (Fig. 4C).

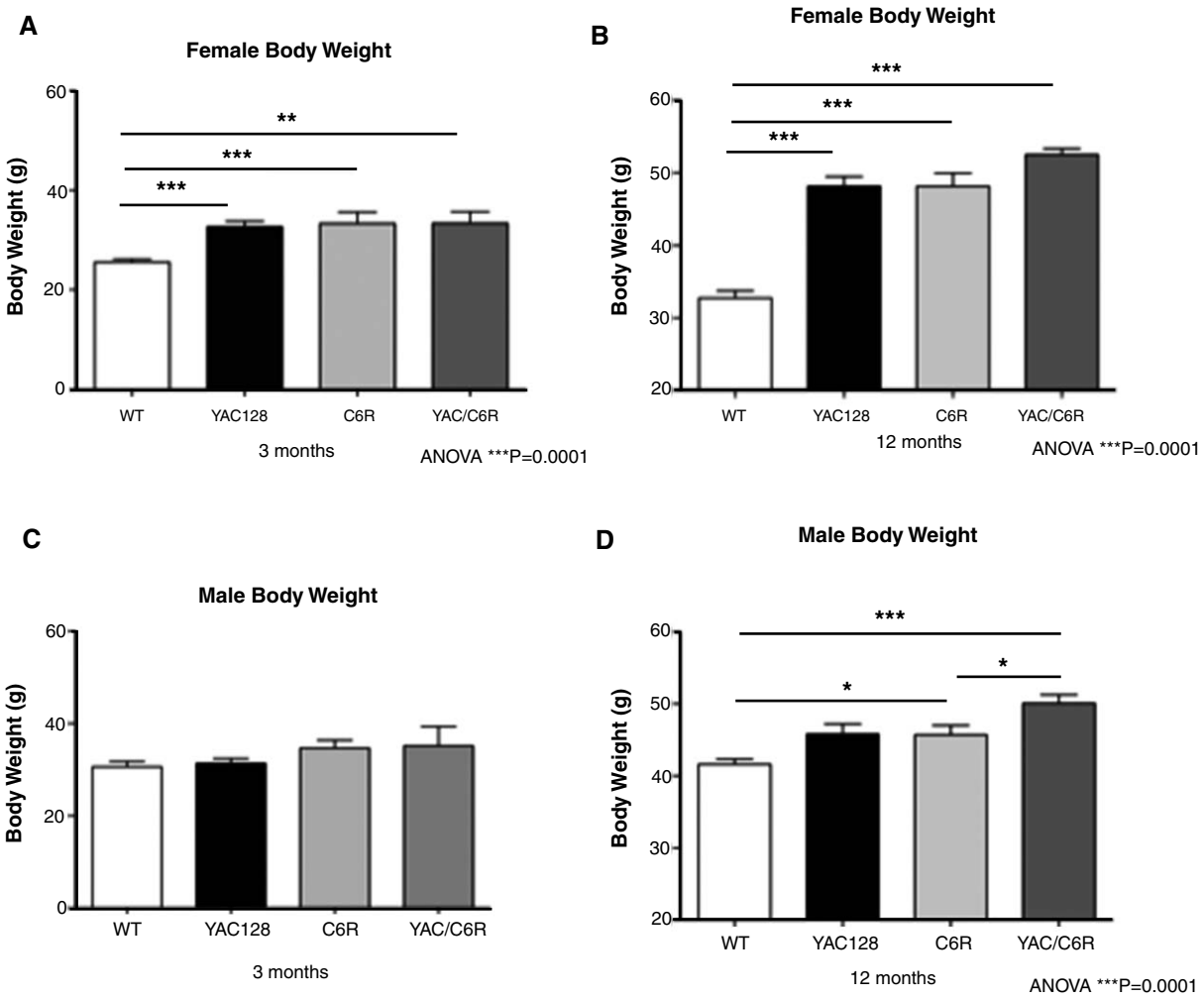


Fig. 3. Body weight is significantly increased in YAC mouse models and influenced by levels of htt. Evaluation of body weight in all genotypes from the cross (WT, YAC128, C6R and YAC/C6R) reveals that female body weights in the transgenic mice at A) 3 and B) 12 month of age demonstrate a significant increase compared to WT (3 months: ANOVA $p = 0.0001$; 12 months: ANOVA $p = 0.0001$). C) No difference in male body weights were observed at 3 months of age in the transgenic YAC vs. WT mice. D) At 12 months of age, male body weights in the YAC mice are significantly higher than WT (ANOVA $p = 0.0001$). *$p < 0.05$; **$p < 0.01$; ***$p < 0.001$.

### *YAC/C6R mice demonstrate striatal neurodegeneration*

In order to examine the effect of concurrently expressing both caspase-cleavable mhtt and C6R mhtt *in vivo* on the selective neuropathological phenotype observed in the YAC128 mice, we assessed brain weight and striatal volume in WT, YAC128, C6R and YAC/C6R mice at 12 months of age ($n = 11$). We have previously defined striatal volume loss as our most robust morphologic endpoint in the YAC128 mice [9, 57, 70]. As expected, YAC128 brain weights are significantly lower than WT controls at 12 months of age (WT = $0.37 \pm 0.01$ g, YAC128 = $0.35 \pm 0.01$ g, $p = 0.02$; Fig. 5A). Similarly, striatal volume is reduced by 12% in YAC128 mice relative to WT controls (WT = $12.7 \pm 0.11$ mm$^3$, YAC128 = $11.2 \pm 0.15$ mm$^3$; $p = 0.003$; Fig. 5B). By contrast, C6R mice do not exhibit a significant reduction in brain weight (C6R = $0.37 \pm 0.01$ g, $p = 0.35$; Fig. 5A) or striatal volume at 12 months compared to WT mice (C6R = $12.3 \pm 0.07$ mm$^3$, $p = 0.33$; Fig. 5B) as found previously [9]. In mice expressing YAC/C6R mhtt a significant decrease in brain weight (YAC/C6R = $0.35 \pm 0.01$ g, $p = 0.007$; Fig. 5A) and striatal volume is observed (YAC/C6R = $10.7 \pm 0.16$ mm$^3$, $p = 0.0019$; Fig. 5B) compared to WT (comparison of all four genotypes,

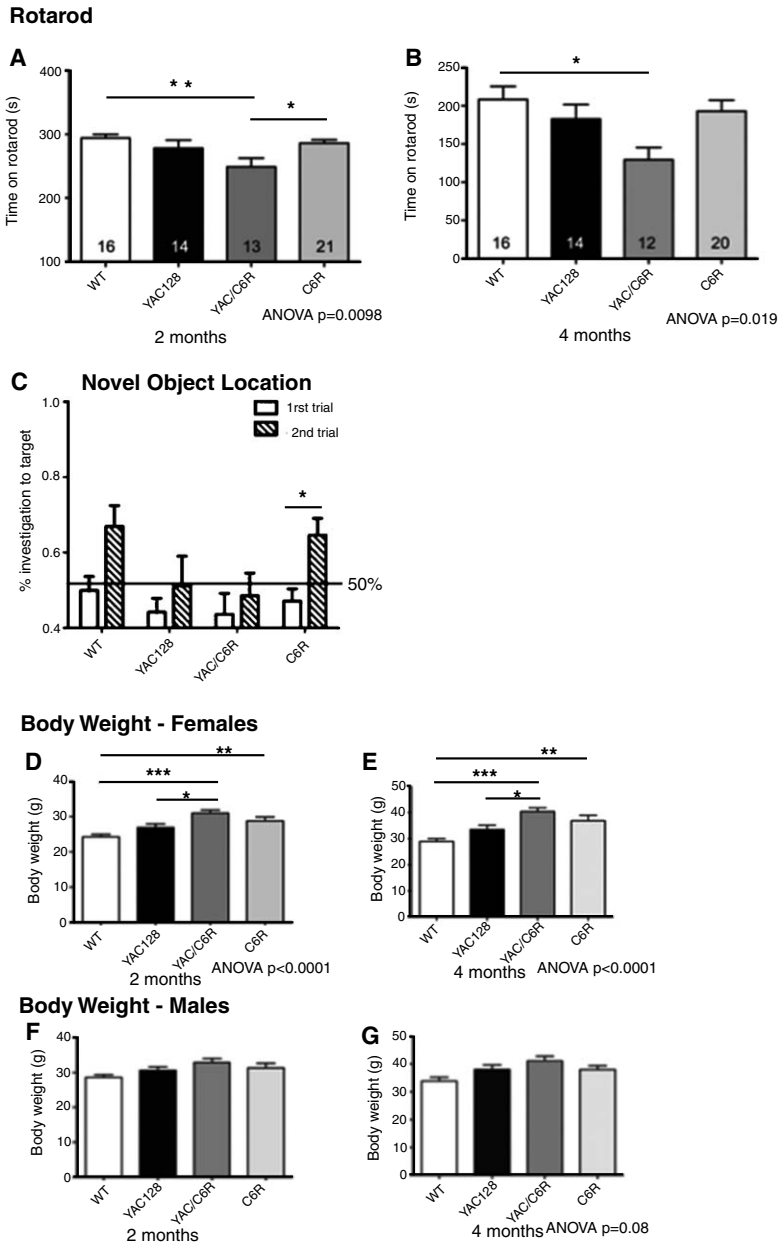


Fig. 4. Motor abnormalities and impaired spatial learning are observed in YAC/C6R mice. A) At 2 and B) 4 months of age rotarod deficits are observed in mice expressing YAC/C6R mhtt (2 months ANOVA $p = 0.009$, WT vs. YAC/C6R $p < 0.01$, C6R vs. YAC/C6R $p < 0.05$; 4 months ANOVA $p < 0.019$, WT vs. YAC/C6R $p < 0.05$). C) To assess spatial learning by preference for a known object in a novel location, 4 month old mice were habituated to an open field for 5 minutes. Mice were then removed from the box for a 5 min ITI and then exposed to novel objects in the open field (T1). Investigations of the novel objects was scored. Mice were then removed from the box for a 5 min ITI, and the object at the top right corner of the box moved to the lower right corner of the box. Mice were then reintroduced to the box and recorded for 5 min during which the frequency and duration of investigations of the objects was scored (T2). A score of 50% indicates no preference. WT and C6R mice display a preference for the novel object location (two-way ANOVA, genotype $p = 0.04$; $F = 2.73$, Bonferroni *post hoc* C6R trial 1 vs. trial 2 $p < 0.05$; WT not significant by *post hoc* but are by *t*-test $p = 0.017$). In contrast, YAC128 and YAC/C6R mice display no preference in either trial indicating impaired spatial learning. $N = 16$ WT mice, 14 YAC128 mice, 12 YAC/C6R mice and 20 C6R mice. Evaluation of body weight in mice used in the early behavior studies (WT, YAC128, C6R and YAC/C6R) reveals that female body weights in the transgenic mice at D) 2 and E) 4 month of age demonstrate a significant increase compared to WT (2 months: ANOVA $p < 0.0001$; 4 months: ANOVA $p < 0.0001$). F) No difference in male body weights were observed at 2 months of age in the transgenic YAC vs. WT mice. G) At 4 months of age, there is a trend towards increased male body weight in the YAC mice vs. WT (ANOVA $p = 0.08$). $^*p < 0.05$; $^{**}p < 0.01$; $^{***}p < 0.001$.

brain: ANOVA $p = 0.003$; striatal volume ANOVA $p = 0.0012$). No difference in cerebellar weight was observed in any of the transgenic mice compared to WT (Fig. 5C).

*Decreased levels of DARPP-32 and increased nuclear htt in YAC/C6R mice*

Levels of DARPP-32 are decreased in HD human postmortem brain tissue and in several HD murine models including the YAC128 mice [38, 73, 74]. We therefore assessed levels of DARPP-32 to further validate the neurodegeneration observed in the YAC/C6R mice ($n = 7$). As found previously, YAC128 mice demonstrate a significant decrease in striatal DARPP-32 levels vs WT ($p = 0.04$, Fig. 6A and B). A trend towards decreased DARPP-32 levels is observed in the YAC/C6R mice ($p = 0.11$, Fig. 6A and B). In contrast, mice expressing C6R mhtt do not demonstrate a decrease in striatal DARPP-32 levels vs. WT ($p = 0.78$, Fig. 6A and B), similar to previous results [38].

Relocation of htt to the nucleus and formation of inclusions area hallmark of the human disease and are present in the brains of human patients [75, 76]. However, since the initial discovery of htt inclusions, there has been continued controversy over the role of htt inclusions/aggregates in the pathogenesisof the disease. Mhtt does have a dose dependent effect on the time course, frequency of htt inclusions and nuclear localization of htt [58]. Similar to HD human post mortem brain tissue, YAC128 mice demonstrate intranuclear striatal inclusions albeit at a low level and late in the phenotype [57, 77]. In contrast to the YAC128 mice, YAC128-shortstop mice exhibit widespread htt inclusions yet do not manifest an HD-related phenotype [77]. Assessment of EM48 immunostaining in the YAC/C6R striatum (Fig. 7A, D) and cortex (Fig. 7B, E) reveals an increase in nuclear htt and inclusions compared to YAC128 or C6R mice (striatum, $n = 3$, ANOVA $p = 0.0004$; cortex, $n = 3$, ANOVA $p = 0.002$) consistent with the increased expression levels of mhtt in these mice. Expression levels of EM48 in YAC128 and C6R mice were as found previously [9, 67].

## DISCUSSION

In this study our goal was to determine whether the neuroprotection observed in mice expressing C6R mhtt is due to dominant negative effects. This was an experiment, in the most classical sense, of a dominant negative mutation study (inserting a mutation or an aa alteration in a protein to elucidate the function of a protein and determine if over expression of the altered polypeptide disrupts the function of the wild type gene) [78]. It is important to clarify that in this experiment we are comparing the effect of mutagenesis of the 586aa site on the function of mutant huntingtin. Motor abnormalities and cognitive deficits, as defined by rotarod performance and preference for a known novel object in a novel location, and striatal neurodegeneration are present in mice concurrently expressing C6R and caspase-cleavable mhtt. This evidence suggests that dominant negative affects do not account for the lack of an HD phenotype in the C6R mice.

In such a study as we describe here, it is first important to rule out other factors that may influence the lack of an observable phenotype in the C6R mice. The phenotype of HD is influenced by mhtt levels and CAG size. Neuroimaging results demonstrate more extensive and severe progressive brain atrophy in the homozygotes and analysis of HD stage (grade) and mean duration showed a shift to the left in the HD homozygotes compared to the heterozygotes individuals [62]. Furthermore, we have demonstrated that onset and progression of the HD phenotype in the YAC128 mouse models is directly modulated by levels of mhtt [58]. Studies in other HD models also support a mhtt dosage effect on the phenotype [64, 79, 80]. HD knock-in mice demonstrate earlier onset of nuclear htt fragment accumulation and a more severe behavioral deficit in the homozygote [81, 82]. In addition to other poly (CAG) disorders (including DRPLA, SCA2, SCA3, SCA6, SCA17), dosage effects are also observed in familial hypercholesterolemia, Parkinson disease and Pelizaeus-Mersbacher disease [83–89]. If mhtt transgene levels were decreased in the C6R mice compared to the YAC128 lines this may erroneously suggest they are protected. Using several markers of transgene expression levels we demonstrate that the C6R mice contain mhtt transgene levels comparable to the YAC128-HD53 line. Furthermore, we have previously demonstrated that HD phenotypes are also present in the lower mhtt expressing lines YAC128-HD55 and HD54 [58]. This evidence demonstrates that dosage effects are not responsible for the neuroprotection observed in the C6R mice.

CAG size is also a critical determinant of the severity of the HD phenotype. Indeed, several neurodegenerative diseases, including spinal bulbar muscular atrophy, dentatorubralpallidoluysian atrophy, Machado-Joseph disease among others are caused by a CAG expansion in their respective protein and a correlation observed between CAG tract length and severity of disease

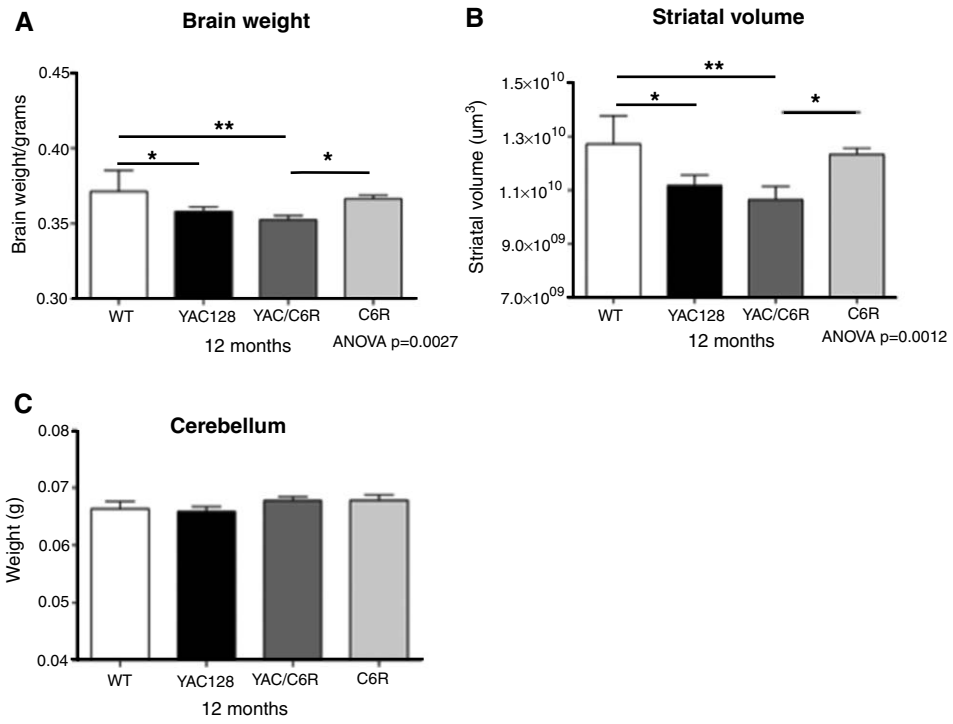


Fig. 5. Neurodegeneration is observed in mice expressing both caspase-cleavable and caspase-6-resistant mhtt (YAC/C6R). A) YAC128 and YAC/C6R brain weights are significantly lower than WT controls at 12 months of age ($n = 11$, WT = $0.37 \pm 0.01$ g, YAC128 = $0.35 \pm 0.01$ g, $p = 0.02$; YAC/C6R = $0.35 \pm 0.01$ g, $p = 0.007$). By contrast, C6R mice do not exhibit a significant reduction in brain weight vs. WT ($n = 11$, C6R = $0.37 \pm 0.01$ g, $p = 0.35$). B) Striatal volume is reduced by 12% in YAC128 mice and 16% in YAC/C6R mice relative to WT controls ($n = 11$, WT = $12.7 \pm 0.11$ mm$^3$, YAC128 = $11.2 \pm 0.15$ mm$^3$; $p = 0.003$; YAC/C6R = $10.7 \pm 0.16$ mm$^3$, $p = 0.0019$). C6R mice do not exhibit a significant reduction in striatal volume at 12 months compared to WT mice ($n = 11$, C6R = $12.3 \pm 0.07$ mm$^3$, $p = 0.33$). Comparison of all four genotypes, brain: ANOVA $p = 0.003$; striatal volume ANOVA $p = 0.0012$. C) No difference in cerebellar weight is observed in any of the transgenic mice compared to WT ($n = 11$). *$p < 0.05$; **$p < 0.01$.

[90–92]. In HD, correlations between CAG repeat length and mitochondrial ADP uptake [93], striatal active casp6 levels [2] and body weight [94] are also detected. As the C6R mice contain a larger CAG size then the YAC128 lines [9] this does not account for the lack of a phenotype in the C6R mice and rather provides additional evidence that cleavage at the 586aa site in mhtt is an important event in the pathogenesis of HD. Another factor, which may influence the lack of a phenotype in the C6R mice, is if the mutated 586aa IVLD site in mhtt (and now present as IVLA in the C6R mice) has altered the conformation of htt and there by altered its function. However, this would appear unlikely as C6R mhtt can rescue the embryonic lethality observed in htt-/- mice demonstrating that mutagenesis of the caspase sites in mhtt does not impair htt function *in vivo* during development [9]. Furthermore, body weight patterns in mice overexpressing htt (either wild type htt, caspase-cleavable or C6R mhtt forms) are similar [68, 69].

In general, much of the knowledge on the mechanisms underlying protein function are derived from gene knock out studies and characterization of artificial or natural occurring alternative and/or mutant forms of a protein. Whereas dominant negative studies in the past have used alternative forms of the wild type protein in order to investigate the function of the protein, here we compared alternative forms of the mutant, polyglutamine expanded, htt protein. Mutating the 586aa IVLD site in mhtt to IVLA and characterization of mice expressing C6R mhtt has provided insights into the underlying neurotoxic mechanisms of caspase-cleavable mhtt [2, 9, 37–39, 67]. An *in vivo* comparison of mice expressing caspase-cleavable mhtt compared to mice expressing C6R mhtt demonstrates alteration of the IVLD site in mhtt has shifted the neurotoxicity of mhtt towards neuroprotection. In the present experiment we wished to determine if the HD phenotypes, observed in mice expressing caspase-cleavable mhtt, are altered with the concurrent expression of mhtt that

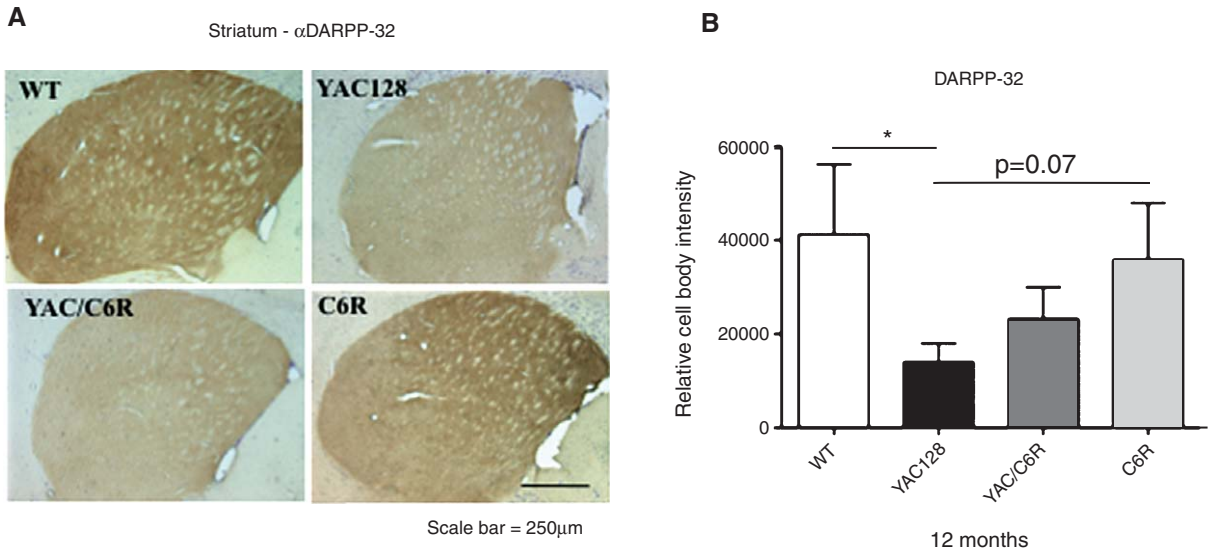


Fig. 6. Decreased DARPP-32 levels in YAC128 striatum A) Photographs of representative DARPP-32 immunostained brains sections from WT, YAC128, YAC/C6R and C6R mice at 12 months of age demonstrate a reduction of DARPP-32 expression in YAC128 striatum compared to WT. Scale bar = 250 μM. B) Quantification of relative cell body staining intensity confirms a significant decrease in levels of DARPP-32 in YAC128 striatum vs. WT mice ($n = 7$, $p = 0.04$). A trend towards decreased DARPP-32 levels is observed in the YAC/C6R mice ($n = 7$, $p = 0.11$). In contrast, mice expressing C6R mhtt do not demonstrate a decrease in striatal DARPP-32 levels vs. WT ($n = 7$, $p = 0.78$). *$p < 0.05$.

expresses a mutation at the 586aa site (D586A) in order to rule out dominant negative effects. A potential caveat of the present study is that YAC128 homozygotes were not used as the control line in order to more effectively control for levels of transgene expression in the YAC/C6R mice. Both naturally occurring and artificially constructed dominant negative mutations have been described. The end effect is disruption and/or inactivation of the wild type gene product. In some cases it is a truncated version of the protein that antagonizes the function of the full-length form. Examples include proteolytic cleavage of NF-κß and/or NR2A. In the case of NF-κß, caspase cleavage generates a transcriptionally inactive p65 molecule still able to bind DNA [15]. Similarly, calpain mediated cleavage of NR2A results in a truncated fragment that is stable and able to interact with NR1 but lacks the structural domain required for scaffolding and downstream signaling [23]. Several diseases are due to antimorphic or dominant negative mutations and include familial neurohypophyseal diabetes insipidus, a number of endocriopathies and marfan syndrome among others [95–97]. Dominant negative effects have also been described in HD. EM48+ inclusions are only observed in the presence of mhtt and thus are markers of the disease in human HD brain and in acute and chronic models of the disease [57, 76, 98]. As wild type htt is sequestered in the inclusions it has been suggested that expression of mhtt may antagonize wild type htt function [99].

It is important to note that *in vivo* expression of C6R mhtt, rather than demonstrating neurotoxicity as observed with caspase-cleavable mhtt, appears to demonstrate similar neuroprotective properties as wild type htt. Indeed, similar resistance to excitotoxic stress and staurosporine treatment are observed in neurons expressing C6R mhtt or YAC18 wild type htt [9, 63, 73]. Furthermore, while phosphorylation levels of htt are decreased in YAC128 striatal tissue, levels are similar in C6R and YAC18 brain tissue [38]. While the mechanism(s) underlying the neuroprotective phenotype in mice/neurons overexpressing wild type htt is currently unknown, a role for htt as a caspase inhibitor has been demonstrated [100, 101]. Interestingly, *in vivo* expression of C6R mhtt also attenuates caspase activation [2]. However the result of the present study would suggest that C6R mhtt is neuroprotective not because mutation of the IVLD site (D586A) has conferred novel properties to this form of mhtt (i.e. caspases inhibition and that C6R mhtt is acting as a caspase sink). However, a caveat of this study is that it cannot be ruled out that caspase-cleavable mhtt is more toxic than C6R mhtt is neuroprotective. If caspase-cleavable mhttt has increased kinetics, of as an example, casp6 activation and/or excitotoxic signaling pathways, this may mask a potentially slower rate of neuroprotective kinetics

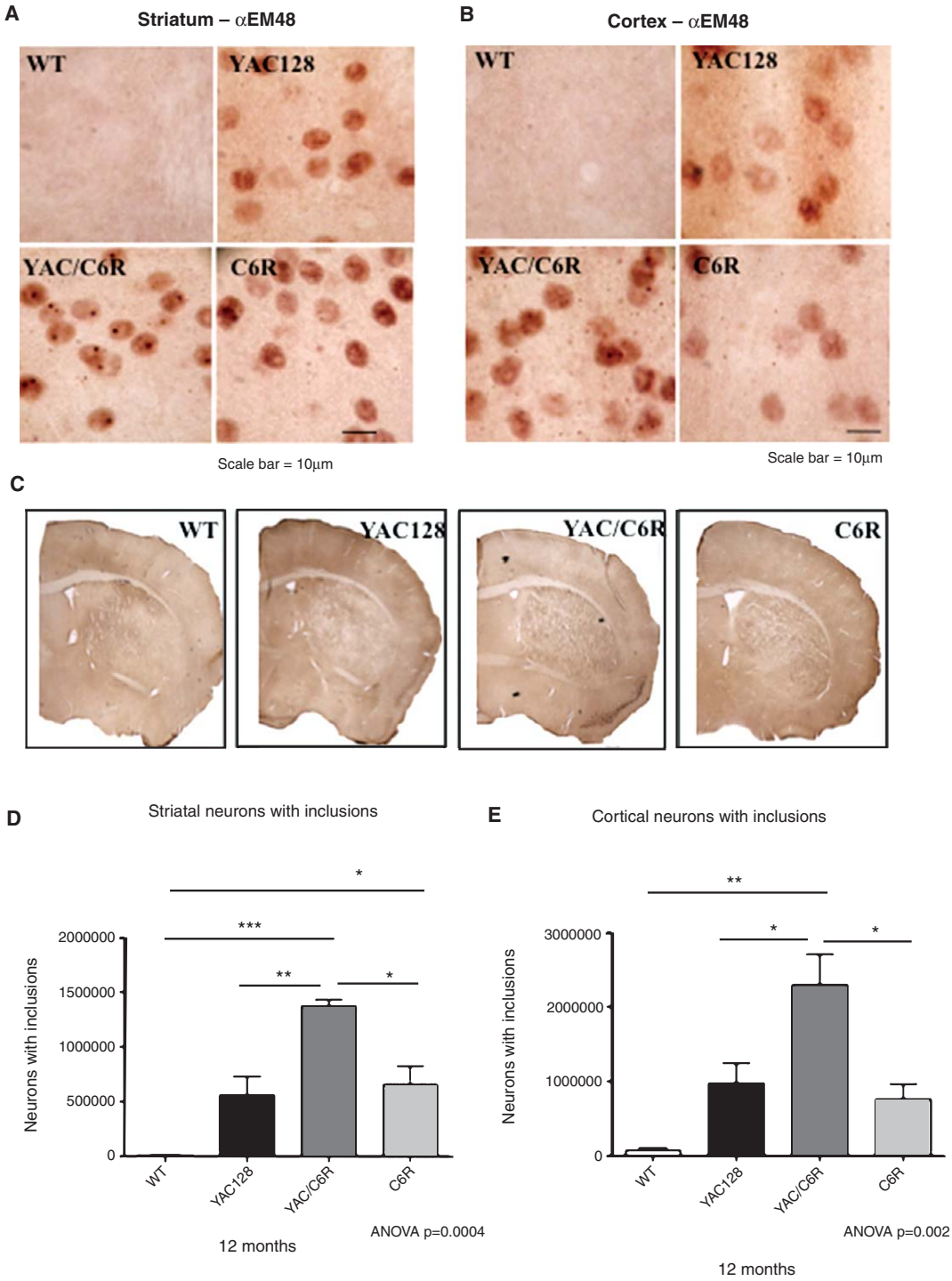


Fig. 7. YAC mouse models demonstrate increased EM48-positive inclusions. Photographs of EM48 immunostained brain sections from WT, YAC128, YAC/C6R and C6R mice at 12 months of age demonstrate an increase in A) striatal and B) cortical EM48-positive inclusions in YAC mice compared to WT mice. C) An overview of brain sections immunostained with EM48 is included for comparison. Quantification of EM48 immunostaining reveals a significant increase in htt inclusions in D) YAC/C6R striatum vs. WT (striatum, $n=3$, ANOVA $p=0.0004$; WT vs. YAC/C6R, $p<0.001$; WT vs. C6R, $p<0.05$; YAC128 vs. YAC/C6R, $p<0.01$; C6R vs. YAC/C6R, $p<0.05$) and E) YAC/C6R cortex compared to WT ($n=3$, ANOVA $p=0.002$; WT vs. YAC/C6R, $p<0.01$; YAC128 vs.YAC/C6R, $p<0.05$; C6R vs. YAC/C6R, $p<0.05$). *$p<0.05$; **$p<0.01$; ***$p<0.001$.

of C6R mhtt (i.e. caspase inhibition). It is interesting to note that some HD phenotypes, observed in the BACHD mouse model, show rescue on a constitutive casp6-/- background and reduced levels of the 586aa htt fragment as detected by immunohistochemistry [27]. These include rescue of rotarod deficits, decreased ubiquitination of proteins and S830 immunopositive aggregates, an antibody known to correlate with overt clinical phentoptye in several mouse models of HD [102–104]. Furthermore, increased clearance of mhtt was observed. These data support a clear role for casp6 in HD and indeed in modulating steady state levels of htt.

Using striatal volume as a primary endpoint we show that neurodegeneration is observed in mice expressing both caspase-cleavable and C6R mhtt concurrently. Neuronal dysfunction, as determined by behavior testing, is also observed in the YAC/C6R mice. These data suggest that it is the direct effect of cleaving mhtt at aa586 that results in the neurotoxicity observed in the YAC128 mouse model of HD and that dominant negative effects do not account for the lack of a phenotype in the C6R mice.

## ACKNOWLEDGMENTS

This work was supported by grants from the CHDI [TREAT-HD], Huntington disease Society of America [20R69538], Canadian Institute of Health Research [CGD-85375].M.R.H, is a Killam University Professor and holds a Canada Research Chair in Human Genetics.D.E is supported by a CIHR post doctoral fellowship. We thank Dr. Paul Greengard and Dr. HughHemming for the kind gift of the DARPP32 antibody, and Xiao Jiang Li for the EM48 antibody.

## CONFLICT OF INTEREST

The authors state no conflict of interest.

## REFERENCES

[1] Novak MJ, Tabrizi SJ. Huntington's disease. BMJ. 2010;340:c3109.

[2] Graham RK, Deng Y, Carroll J, Vaid K, Cowan C, Pouladi MA, Metzler M, Bissada N, Wang L, Faull RL, Gray M, Yang XW, Raymond LA, Hayden MR. Cleavage at the 586 amino acid caspase-6 site in mutant huntingtin influences caspase-6 activation *in vivo*. J Neurosci. 2010;30:15019-29.

[3] Hermel E, Gafni J, Propp SS, Leavitt BR, Wellington CL, Young JE, Hackam AS, Logvinova AV, Peel AL, Chen SF, Hook V, Singaraja R, Krajewski S, Goldsmith PC, Ellerby HM, Hayden MR, Bredesen DE, Ellerby LM. Specific caspase interactions and amplification are involved in selective neuronal vulnerability in Huntington's disease. Cell Death Differ. 2004;11:424-38.

[4] Vis JC, Schipper E, de Boer-van Huizen RT, Verbeek MM, de Waal RM, Wesseling P, ten Donkelaar HJ, Kremer B. Expression pattern of apoptosis-related markers in Huntington's disease. Acta Neuropathol. 2005;109:321-8.

[5] Kiechle T, Dedeoglu A, Kubilus J, Kowall NW, Beal MF, Friedlander RM, Hersch SM, Ferrante RJ. Cytochrome C and caspase-9 expression in Huntington's disease. Neuromolecular Med. 2002;1:183-95.

[6] Dragunow M, Faull RL, Lawlor P, Beilharz EJ, Singleton K, Walker EB, Mee E. *In situ* evidence for DNA fragmentation in Huntington's disease striatum and Alzheimer's disease temporal lobes. Neuroreport. 1995;6:1053-7.

[7] Goldberg YP, Nicholson DW, Rasper DM, Kalchman MA, Koide HB, Graham RK, Bromm M, Kazemi-Esfarjani P, Thornberry NA, Vaillancourt JP, Hayden MR. Cleavage of huntingtin by apopain, a proapoptotic cysteine protease, is modulated by the polyglutamine tract. Nat Genet. 1996;13:442-9.

[8] Wellington CL, Ellerby LM, Hackam AS, Margolis RL, Trifiro MA, Singaraja R, McCutcheon K, Salvesen GS, Propp SS, Bromm M, Rowland KJ, Zhang T, Rasper D, Roy S, Thornberry N, Pinsky L, Kakizuka A, Ross CA, Nicholson DW, Bredesen DE, Hayden MR. Caspase cleavage of gene products associated with triplet expansion disorders generates truncated fragments containing the polyglutamine tract. J Biol Chem. 1998;273:9158-67.

[9] Graham RK, Deng Y, Slow EJ, Haigh B, Bissada N, Lu G, Pearson J, Shehadeh J, Bertram L, Murphy Z, Warby SC, Doty CN, Roy S, Wellington CL, Leavitt BR, Raymond LA, Nicholson DW, Hayden MR. Cleavage at the caspase-6 site is required for neuronal dysfunction and degeneration due to mutant huntingtin. Cell. 2006;125:1179-91.

[10] Wellington CL, Ellerby LM, Gutekunst CA, Rogers D, Warby S, Graham RK, Loubser O, van Raamsdonk J, Singaraja R, Yang YZ, Gafni J, Bredesen D, Hersch SM, Leavitt BR, Roy S, Nicholson DW, Hayden MR. Caspase cleavage of mutant huntingtin precedes neurodegeneration in Huntington's disease. J Neurosci. 2002;22:7862-72.

[11] Wellington CL, Singaraja R, Ellerby L, Savill J, Roy S, Leavitt B, Cattaneo E, Hackam A, Sharp A, Thornberry N, Nicholson DW, Bredesen DE, Hayden MR. Inhibiting caspase cleavage of huntingtin reduces toxicity and aggregate formation in neuronal and nonneuronal cells. J Biol Chem. 2000;275:19831-8.

[12] Mangiarini L, Sathasivam K, Seller M, Cozens B, Harper A, Hetherington C, Lawton M, Trottier Y, Lehrach H, Davies SW, Bates GP. Exon 1 of the HD gene with an expanded CAG repeat is sufficient to cause a progressive neurological phenotype in transgenic mice. Cell. 1996;87:493-506.

[13] Hackam AS, Singaraja R, Wellington CL, Metzler M, McCutcheon K, Zhang T, Kalchman M, Hayden MR. The influence of huntingtin protein size on nuclear localization and cellular toxicity. J Cell Biol. 1998;141:1097-105.

[14] Kim YJ, Yi Y, Sapp E, Wang Y, Cuiffo B, Kegel KB, Qin ZH, Aronin N, DiFiglia M. Caspase 3-cleaved N-terminal fragments of wild-type and mutant huntingtin are present in normal and Huntington's disease brains, associate with membranes, and undergo calpain-dependent proteolysis. Proc Natl Acad Sci U S A. 2001;98:12784-9.

[15] Levkau B, Scatena M, Giachelli CM, Ross R, Raines EW. Apoptosis overrides survival signals through a caspase-mediated dominant-negative NF-kappa B loop. Nat Cell Biol. 1999;1:227-33.

[16] Mazars A, Fernandez-Vidal A, Mondesert O, Lorenzo C, Prevost G, Ducommun B, Payrastre B, Racaud-Sultan C, Manenti S. A caspase-dependent cleavage of CDC25A generates an active fragment activating cyclin-dependent kinase 2 during apoptosis. Cell Death Differ. 2009;16:208-18.

[17] de Calignon A, Fox LM, Pitstick R, Carlson GA, Bacskai BJ, Spires-Jones TL, Hyman BT. Caspase activation precedes and leads to tangles. Nature. 2010;464:1201-4.

[18] Halawani D, Tessier S, Anzellotti D, Bennett DA, Latterich M, LeBlanc AC. Identification of Caspase-6-mediated processing of the valosin containing protein (p97) in Alzheimer's disease: A novel link to dysfunction in ubiquitin proteasome system-mediated protein degradation. J Neurosci. 2010;30:6132-42.

[19] Chan YW, Chen Y, Poon RY. Generation of an indestructible cyclin B1 by caspase-6-dependent cleavage during mitotic catastrophe. Oncogene. 2009;28:170-83.

[20] Tang G, Yang J, Minemoto Y, Lin A. Blocking caspase-3-mediated proteolysis of IKKbeta suppresses TNF-alpha-induced apoptosis. Mol Cell. 2001;8:1005-16.

[21] Breckenridge DG, Stojanovic M, Marcellus RC, Shore GC. Caspase cleavage product of BAP31 induces mitochondrial fission through endoplasmic reticulum calcium signals, enhancing cytochrome C release to the cytosol. J Cell Biol. 2003;160:1115-27.

[22] Robert G, Puissant A, Dufies M, Marchetti S, Jacquel A, Cluzeau T, Colosetti P, Belhacene N, Kahle P, Da Costa CA, Luciano F, Checler F, Auberger P. The caspase 6 derived N-terminal fragment of DJ-1 promotes apoptosis via increased ROS production. Cell Death Diff. 2012;19:1769-78.

[23] Gascon S, Sobrado M, Roda JM, Rodriguez-Pena A, Diaz-Guerra M. Excitotoxicity and focal cerebral ischemia induce truncation of the NR2A and NR2B subunits of the NMDA receptor and cleavage of the scaffolding protein PSD-95. Mol psychiatry. 2008;13:99-114.

[24] Tebbenkamp AT, Green C, Xu G, Denovan-Wright EM, Rising AC, Fromholt SE, Slunt HH, Swing D, Mandel RJ, Tessarollo L, Borchelt DR. Transgenic mice expressing caspase-6 derived N-terminal fragments of mutant huntingtin develop neurologic abnormalities with predominant cytoplasmic inclusion pathology composed largely of a smaller proteolytic derivative. Hum Mol Genet. 2011;20:2770-82.

[25] Landles C, Sathasivam K, Weiss A, Woodman B, Moffitt H, Finkbeiner S, Sun B, Gafni J, Ellerby LM, Trottier Y, Richards WG, Osmand A, Paganetti P, Bates GP. Proteolysis of mutant huntingtin produces an exon 1 fragment that accumulates as an aggregated protein in neuronal nuclei in Huntington disease. J Biol Chem. 2010;285:8808-23.

[26] Waldron-Roby E, Ratovitski T, Wang X, Jiang M, Watkin E, Arbez N, Graham RK, Hayden MR, Hou Z, Mori S, Swing D, Pletnikov M, Duan W, Tessarollo L, Ross CA. Transgenic mouse model expressing the caspase 6 fragment of mutant huntingtin. J Neurosci. 2012;32:183-93.

[27] Gafni J, Papanikolaou T, Degiacomo F, Holcomb J, Chen S, Menalled L, Kudwa A, Fitzpatrick J, Miller S, Ramboz S, Tuunanen PI, Lehtimaki KK, Yang XW, Park L, Kwak S, Howland D, Park H, Ellerby LM. Caspase-6 activity in a BACHD mouse modulates steady-state levels of mutant huntingtin protein but is not necessary for production of a 586 amino acid proteolytic fragment. J Neurosci. 2012;32:7454-65.

[28] Guo H, Albrecht S, Bourdeau M, Petzke T, Bergeron C, LeBlanc AC. Active caspase-6 and caspase-6-cleaved tau in neuropil threads, neuritic plaques, and neurofibrillary tangles of Alzheimer's disease. Am J Pathol. 2004;165:523-31.

[29] Albrecht S, Bourdeau M, Bennett D, Mufson EJ, Bhattacharjee M, LeBlanc AC. Activation of caspase-6 in aging and mild cognitive impairment. Am J Pathol. 2007;170:1200-9.

[30] Gervais FG, Xu D, Robertson GS, Vaillancourt JP, Zhu Y, Huang J, LeBlanc A, Smith D, Rigby M, Shearman MS, Clarke EE, Zheng H, Van Der Ploeg LH, Ruffolo SC, Thornberry NA, Xanthoudakis S, Zamboni RJ, Roy S, Nicholson DW. Involvement of caspases in proteolytic cleavage of Alzheimer's amyloid-beta precursor protein and amyloidogenic A beta peptide formation. Cell. 1999;97:395-406.

[31] LeBlanc A, Liu H, Goodyer C, Bergeron C, Hammond J. Caspase-6 role in apoptosis of human neurons, amyloidogenesis, and Alzheimer's disease. J Biol Chem. 1999;274:23426-36.

[32] Galvan V, Chen S, Lu D, Logvinova A, Goldsmith P, Koo EH, Bredesen DE. Caspase cleavage of members of the amyloid precursor family of proteins. J Neurochem. 2002;82:283-94.

[33] Zhao M, Su J, Head E, Cotman CW. Accumulation of caspase cleaved amyloid precursor protein represents an early neurodegenerative event in aging and in Alzheimer's disease. Neurobiol Dis. 2003;14:391-403.

[34] Banwait S, Galvan V, Zhang J, Gorostiza OF, Ataie M, Huang W, Crippen D, Koo EH, Bredesen DE. C-terminal cleavage of the amyloid-beta protein precursor at Asp664: A switch associated with Alzheimer's disease. J Alzheimers Dis. 2008;13:1-16.

[35] Nguyen TV, Galvan V, Huang W, Banwait S, Tang H, Zhang J, Bredesen DE. Signal transduction in Alzheimer disease: p21-activated kinase signaling requires C-terminal cleavage of APP at Asp664. J Neurochem. 2008;104:1065-80.

[36] Saganich MJ, Schroeder BE, Galvan V, Bredesen DE, Koo EH, Heinemann SF. Deficits in synaptic transmission and learning in amyloid precursor protein (APP) transgenic mice require C-terminal cleavage of APP. J Neurosci. 2006;26:13428-36.

[37] Pouladi MA, Graham RK, Karasinska JM, Xie Y, Santos RD, Petersen A, Hayden MR. Prevention of depressive behaviour in the YAC128 mouse model of Huntington disease by mutation at residue 586 of huntingtin. Brain: A Journal of Neurology. 2009;132:919-32.

[38] Metzler M, Gan L, Mazarei G, Graham RK, Liu L, Bissada N, Lu G, Leavitt BR, Hayden MR. Phosphorylation of huntingtin at Ser421 in YAC128 neurons is associated with protection of YAC128 neurons from NMDA-mediated excitotoxicity and is modulated by PP1 and PP2A. J Neurosci. 2010;30:14318-29.

[39] Milnerwood AJ, Gladding CM, Pouladi MA, Kaufman AM, Hines RM, Boyd JD, Ko RW, Vasuta OC, Graham RK, Hayden MR, Murphy TH, Raymond LA. Early increase in extrasynaptic NMDA receptor signaling and expression contributes to phenotype onset in Huntington's disease mice. Neuron. 2010;65:178-90.

[40] Galvan V, Gorostiza OF, Banwait S, Ataie M, Logvinova AV, Sitaraman S, Carlson E, Sagi SA, Chevallier N, Jin K, Greenberg DA, Bredesen DE. Reversal of Alzheimer's-like pathology and behavior in human APP transgenic mice by mutation of Asp664. Proc Natl Acad Sci U S A. 2006;103:7130-5.

[41] Galvan V, Zhang J, Gorostiza OF, Banwait S, Huang W, Ataie M, Tang H, Bredesen DE. Long-term prevention

of Alzheimer's disease-like behavioral deficits in PDAPP mice carrying a mutation in Asp664. Behav Brain Res. 2008;191:246-55.

[42] Harris JA, Devidze N, Halabisky B, Lo I, Thwin MT, Yu GQ, Bredesen DE, Masliah E, Mucke L. Many neuronal and behavioral impairments in transgenic mouse models of Alzheimer's disease are independent of caspase cleavage of the amyloid precursor protein. J Neurosci. 2010;30:372-81.

[43] Albrecht S, Bogdanovic N, Ghetti B, Winblad B, LeBlanc AC. Caspase-6 activation in familial Alzheimer disease brains carrying amyloid precursor protein or presenilini or presenilin II mutations. J Neuropathol Exp Neurol. 2009;68:1282-93.

[44] Klaiman G, Petzke TL, Hammond J, LeBlanc AC. Targets of caspase-6 activity in human neurons and Alzheimer disease. Mol Cell Proteomics. 2008;7:1541-55.

[45] Oliver FJ, de la Rubia G, Rolli V, Ruiz-Ruiz MC, de Murcia G, Murcia JM. Importance of poly(ADP-ribose) polymerase and its cleavage in apoptosis. Lesson from an uncleavable mutant. J Biol Chem. 1998;273:33533-9.

[46] Gafni J, Hermel E, Young JE, Wellington CL, Hayden MR, Ellerby LM. Inhibition of calpain cleavage of huntingtin reduces toxicity: Accumulation of calpain/caspase fragments in the nucleus. J Biol Chem. 2004;279:20211-20.

[47] Young JE, Gouw L, Propp S, Sopher BL, Taylor J, Lin A, Hermel E, Logvinova A, Chen SF, Chen S, Bredesen DE, Truant R, Ptacek LJ, La Spada AR, Ellerby LM. Proteolytic cleavage of ataxin-7 by caspase-7 modulates cellular toxicity and transcriptional dysregulation. J Biol Chem. 2007;282:30150-60.

[48] Rao L, Perez D, White E. Lamin proteolysis facilitates nuclear events during apoptosis. J Cell Biol. 1996;135:1441-55.

[49] Charvet C, Alberti I, Luciano F, Jacquel A, Bernard A, Auberger P, Deckert M. Proteolytic regulation of Forkhead transcription factor FOXO3a by caspase-3-like proteases. Oncogene. 2003;22:4557-68.

[50] Wang B, Nguyen M, Breckenridge DG, Stojanovic M, Clemons PA, Kuppig S, Shore GC. Uncleaved BAP31 in association with A4 protein at the endoplasmic reticulum is an inhibitor of Fas-initiated release of cytochrome c from mitochondria. J Biol Chem. 2003;278:14461-8.

[51] Lane JD, Lucocq J, Pryde J, Barr FA, Woodman PG, Allan VJ, Lowe M. Caspase-mediated cleavage of the stacking protein GRASP65 is required for Golgi fragmentation during apoptosis. J Cell Biol. 2002;156:495-509.

[52] Walter J, Schindzielorz A, Grunberg J, Haass C. Phosphorylation of presenilin-2 regulates its cleavage by caspases and retards progression of apoptosis. Proc Natl Acad Sci U S A. 1999;96:1391-6.

[53] D'Costa AM, Denning MF. A caspase-resistant mutant of PKC-delta protects keratinocytes from UV-induced apoptosis. Cell Death Diff. 2005;12:224-32.

[54] Nguyen M, Breckenridge DG, Ducret A, Shore GC. Caspase-resistant BAP31 inhibits fas-mediated apoptotic membrane fragmentation and release of cytochrome c from mitochondria. Mol Cell Biol. 2000;20:6731-40.

[55] Latchoumycandane C, Anantharam V, Kitazawa M, Yang Y, Kanthasamy A, Kanthasamy AG. Protein kinase C delta is a key downstream mediator of manganese-induced apoptosis in dopaminergic neuronal cells. J Pharmacol Exp Ther. 2005;313:46-55.

[56] Assefa Z, Bultynck G, Szlufcik K, Nadif Kasri N, Vermassen E, Goris J, Missiaen L, Callewaert G, Parys JB, De Smedt H. Caspase-3-induced truncation of type 1 inositol trisphosphate receptor accelerates apoptotic cell death and induces inositol trisphosphate-independent calcium release during apoptosis. J Biol Chem. 2004;279:43227-36.

[57] Slow EJ, van RJ, Rogers D, Coleman SH, Graham RK, Deng Y, Oh R, Bissada N, Hossain SM, Yang YZ, Li XJ, Simpson EM, Gutekunst CA, Leavitt BR, Hayden MR. Selective striatal neuronal loss in a YAC128 mouse model of Huntington disease. Hum Mol Genet. 2003;12:1555-67.

[58] Graham RK, Slow EJ, Deng Y, Bissada N, Lu G, Pearson J, Shehadeh J, Leavitt BR, Raymond LA, Hayden MR. Levels of mutant huntingtin influence the phenotypic severity of Huntington disease in YAC128 mouse models. Neurobiol Dis. 2006;21:444-55.

[59] Weiss A, Abramowski D, Bibel M, Bodner R, Chopra V, DiFiglia M, Fox J, Kegel K, Klein C, Grueninger S, Hersch S, Housman D, Regulier E, Rosas HD, Stefani M, Zeitlin S, Bilbe G, Paganetti P. Single-step detection of mutant huntingtin in animal and human tissues: A bioassay for Huntington's disease. Anal Biochem. 2009;395:8-15.

[60] Kalchman MA, Koide HB, McCutcheon K, Graham RK, Nichol K, Nishiyama K, Kazemi-Esfarjani P, Lynn FC, Wellington C, Metzler M, Goldberg YP, Kanazawa I, Gietz RD, Hayden MR. HIP1, a human homologue of S. cerevisiae Sla2p, interacts with membrane-associated huntingtin in the brain. Nat Genet. 1997;16:44-53.

[61] Van Raamsdonk JM, Murphy Z, Slow EJ, Leavitt BR, Hayden MR. Selective degeneration and nuclear localization of mutant huntingtin in the YAC128 mouse model of Huntington disease. Hum Mol Genet. 2005;14:3823-35.

[62] Squitieri F, Gellera C, Cannella M, Mariotti C, Cislaghi G, Rubinsztein DC, Almqvist EW, Turner D, Bachoud-Levi AC, Simpson SA, Delatycki M, Maglione V, Hayden MR, Donato SD. Homozygosity for CAG mutation in Huntington disease is associated with a more severe clinical course. Brain: A Journal of Neurology. 2003;126:946-55.

[63] Shehadeh J, Fernandes HB, Zeron Mullins MM, Graham RK, Leavitt BR, Hayden MR, Raymond LA. Striatal neuronal apoptosis is preferentially enhanced by NMDA receptor activation in YAC transgenic mouse model of Huntington disease. Neurobiol Dis. 2006;21:392-403.

[64] Reddy PH, Williams M, Charles V, Garrett L, Pike-Buchanan L, Whetsell WO Jr, Miller G, Tagle DA. Behavioural abnormalities and selective neuronal loss in HD transgenic mice expressing mutated full-length HD cDNA. Nature genetics. 1998;20:198-202.

[65] Andrew S, Theilmann J, Almqvist E, Norremolle A, Lucotte G, Anvret M, Sorensen SA, Turpin JC, Hayden MR. DNA analysis of distinct populations suggests multiple origins for the mutation causing Huntington disease. Clin Genet. 1993;43:286-94.

[66] Brinkman RR, Mezei MM, Theilmann J, Almqvist E, Hayden MR. The likelihood of being affected with Huntington disease by a particular age, for a specific CAG size. Am J Hum Genet. 1997;60:1202-10.

[67] Wang CE, Tydlacka S, Orr AL, Yang SH, Graham RK, Hayden MR, Li S, Chan AW, Li XJ. Accumulation of N-terminal mutant huntingtin in mouse and monkey models implicated as a pathogenic mechanism in Huntington's disease. Hum Mol Genet. 2008;17:2738-51.

[68] Van Raamsdonk JM, Gibson WT, Pearson J, Murphy Z, Lu G, Leavitt BR, Hayden MR. Body weight is modulated by levels of full-length huntingtin. Hum Mol Genet. 2006;15:1513-23.

[69] Pouladi MA, Xie Y, Skotte NH, Ehrnhoefer DE, Graham RK, Kim JE, Bissada N, Yang XW, Paganetti P, Friedlander

RM, Leavitt BR, Hayden MR. Full-length huntingtin levels modulate body weight by influencing insulin-like growth factor 1 expression. Hum Mol Genet. 2010;19:1528-38.
[70] Van Raamsdonk JM, Pearson J, Slow EJ, Hossain SM, Leavitt BR, Hayden MR. Cognitive dysfunction precedes neuropathology and motor abnormalities in the YAC128 mouse model of Huntington's disease. J Neurosci. 2005;25:4169-80.
[71] Okamoto S, Pouladi MA, Talantova M, Yao D, Xia P, Ehrnhoefer DE, Zaidi R, Clemente A, Kaul M, Graham RK, Zhang D, Vincent Chen HS, Tong G, Hayden MR, Lipton SA. Balance between synaptic versus extrasynaptic NMDA receptor activity influences inclusions and neurotoxicity of mutant huntingtin. Nat Med. 2009;15:1407-13.
[72] Southwell AL, Ko J, Patterson PH. Intrabody gene therapy ameliorates motor, cognitive, and neuropathological symptoms in multiple mouse models of Huntington's disease. J Neurosci. 2009;29:13589-602.
[73] Leavitt BR, Raamsdonk JM, Shehadeh J, Fernandes H, Murphy Z, Graham RK, Wellington CL, Raymond LA, Hayden MR. Wild-type huntingtin protects neurons from excitotoxicity. J Neurochem. 2006;96:1121-9.
[74] Bibb JA, Yan Z, Svenningsson P, Snyder GL, Pieribone VA, Horiuchi A, Nairn AC, Messer A, Greengard P. Severe deficiencies in dopamine signaling in presymptomatic Huntington's disease mice. Proc Natl Acad Sci U S A. 2000; 97:6809-14.
[75] DiFiglia M, Sapp E, Chase K, Schwarz C, Meloni A, Young C, Martin E, Vonsattel JP, Carraway R, Reeves SA. Huntingtin is a cytoplasmic protein associated with vesicles in human and rat brain neurons. Neuron. 1995;14: 1075-81.
[76] Gutekunst CA, Levey AI, Heilman CJ, Whaley WL, Yi H, Nash NR, Rees HD, Madden JJ, Hersch SM. Identification and localization of huntingtin in brain and human lymphoblastoid cell lines with anti-fusion protein antibodies. Proc Natl Acad. Sci U S A. 1995;92:8710-4.
[77] Slow EJ, Graham RK, Osmand AP, Devon RS, Lu G, Deng Y, Pearson J, Vaid K, Bissada N, Wetzel R, Leavitt BR, Hayden MR. Absence of behavioral abnormalities and neurodegeneration *in vivo* despite widespread neuronal huntingtin inclusions. Proc Natl Acad Sci U S A. 2005; 102:11402-7.
[78] Herskowitz I. Functional inactivation of genes by dominant negative mutations. Nature. 1987;329:219-22.
[79] Davies SW, Turmaine M, Cozens BA, DiFiglia M, Sharp AH, Ross CA, Scherzinger E, Wanker EE, Mangiarini L, Bates GP. Formation of neuronal intranuclear inclusions underlies the neurological dysfunction in mice transgenic for the HD mutation. Cell. 1997;90:537-48.
[80] Hodgson JG, Agopyan N, Gutekunst CA, Leavitt BR, LePiane F, Singaraja R, Smith DJ, Bissada N, McCutcheon K, Nasir J, Jamot L, Li XJ, Stevens ME, Rosemond E, Roder JC, Phillips AG, Rubin EM, Hersch SM, Hayden MR. A YAC mouse model for Huntington's disease with full-length mutant huntingtin, cytoplasmic toxicity, and selective striatal neurodegeneration. Neuron. 1999;23:181-92.
[81] Wheeler VC, Gutekunst CA, Vrbanac V, Lebel LA, Schilling G, Hersch S, Friedlander RM, Gusella JF, Vonsattel JP, Borchelt DR, Macdonald ME. Early phenotypes that presage late-onset neurodegenerative disease allow testing of modifiers in Hdh CAG knock-in mice. Hum Mol Genet. 2002;11:633-40.
[82] Lin CH, Tallaksen-Greene S, Chien WM, Cearley JA, Jackson WS, Crouse AB, Ren S, Li XJ, Albin RL, Detloff PJ. Neurological abnormalities in a knock-in mouse model of Huntington's disease. Hum Mol Genet. 2001;10:137-44.
[83] Durr A, Hahn-Barma V, Brice A, Pecheux C, Dode C, Feingold J. Homozygosity in Huntington's disease. Jmed Genet. 1999;36:172-3.
[84] Zlotogora J. Dominance and homozygosity. Am J Med Genet. 1997;68:412-6.
[85] Bilheimer DW, Stone NJ, Grundy SM. Metabolic studies in familial hypercholesterolemia. Evidence for a gene-dosage effect *in vivo*. J Clin Invest. 1979;64:524-33.
[86] Singleton AB, Farrer M, Johnson J, Singleton A, Hague S, Kachergus J, Hulihan M, Peuralinna T, Dutra A, Nussbaum R, Lincoln S, Crawley A, Hanson M, Maraganore D, Adler C, Cookson MR, Muenter M, Baptista M, Miller D, Blancato J, Hardy J, Gwinn-Hardy K. alpha-Synuclein locus triplication causes Parkinson's disease. Science. 2003;302:841.
[87] Nishioka K, Hayashi S, Farrer MJ, Singleton AB, Yoshino H, Imai H, Kitami T, Sato K, Kuroda R, Tomiyama H, Mizoguchi K, Murata M, Toda T, Imoto I, Inazawa J, Mizuno Y, Hattori N. Clinical heterogeneity of alpha-synuclein gene duplication in Parkinson's disease. Ann Neurol. 2006;59:298-309.
[88] Fuchs J, Nilsson C, Kachergus J, Munz M, Larsson EM, Schule B, Langston JW, Middleton FA, Ross OA, Hulihan M, Gasser T, Farrer MJ. Phenotypic variation in a large Swedish pedigree due to SNCA duplication and triplication. Neurology. 2007;68:916-22.
[89] Wolf NI, Sistermans EA, Cundall M, Hobson GM, Davis-Williams AP, Palmer R, Stubbs P, Davies S, Endziniene M, Wu Y, Chong WK, Malcolm S, Surtees R, Garbern JY, Woodward KJ. Three or more copies of the proteolipid protein gene PLP1 cause severe Pelizaeus-Merzbacher disease. Brain: A Journal of Neurology. 2005;128:743-51.
[90] Doyu M, Sobue G, Mukai E, Kachi T, Yasuda T, Mitsuma T, Takahashi A. Severity of X-linked recessive bulbospinal neuronopathy correlates with size of the tandem CAG repeat in androgen receptor gene. Ann Neurol. 1992;32: 707-10.
[91] Atsuta N, Watanabe H, Ito M, Banno H, Suzuki K, Katsuno M, Tanaka F, Tamakoshi A, Sobue G. Natural history of spinal and bulbar muscular atrophy (SBMA): A study of 223 Japanese patients. Brain: A Journal of Neurology. 2006;129:1446-55.
[92] Martin JB. Molecular basis of the neurodegenerative disorders. N Engl J Med. 1999;340:1970-80.
[93] Seong IS, Ivanova E, Lee JM, Choo YS, Fossale E, Anderson M, Gusella JF, Laramie JM, Myers RH, Lesort M, Macdonald ME. HD CAG repeat implicates a dominant property of huntingtin in mitochondrial energy metabolism. Hum Mol Genet. 2005;14:2871-80.
[94] Aziz NA, van der Burg JM, Landwehrmeyer GB, Brundin P, Stijnen T, Group ES, Roos RA. Weight loss in Huntington disease increases with higher CAG repeat number. Neurology. 2008;71:1506-13.
[95] Russell TA, Ito M, Ito M, Yu RN, Martinson FA, Weiss J, Jameson JL. A murine model of autosomal dominant neurohypophyseal diabetes insipidus reveals progressive loss of vasopressin-producing neurons. J Clin Inves. 2003;112:1697-706.
[96] Phillips JA 3rd. Dominant-negative diabetes insipidus and other endocrinopathies. J Clin Invest. 2003;112:1641-3.
[97] Faivre L, Collod-Beroud G, Loeys BL, Child A, Binquet C, Gautier E, Callewaert B, Arbustini E, Mayer K, Arslan-Kirchner M, Kiotsekoglou A, Comeglio P, Marziliano N,

Dietz HC, Halliday D, Beroud C, Bonithon-Kopp C, Claustres M, Muti C, Plauchu H, Robinson PN, Ades LC, Biggin A, Benetts B, Brett M, Holman KJ, De Backer J, Coucke P, Francke U, De Paepe A, Jondeau G, Boileau C. Effect of mutation type and location on clinical outcome in 1,013 probands with Marfan syndrome or related phenotypes and FBN1 mutations: An international study. Am J Hum Genet. 2007;81:454-66.

[98] DiFiglia M, Sapp E, Chase KO, Davies SW, Bates GP, Vonsattel JP, Aronin N. Aggregation of huntingtin in neuronal intranuclear inclusions and dystrophic neurites in brain. Science. 1997;277:1990-3.

[99] Huang CC, Faber PW, Persichetti F, Mittal V, Vonsattel JP, MacDonald ME, Gusella JF. Amyloid formation by mutant huntingtin: Threshold, progressivity and recruitment of normal polyglutamine proteins. Somat Cell Mol Genet. 1998;24:217-33.

[100] Zhang Y, Leavitt BR, Van Raamsdonk JM, Dragatsis I, Goldowitz D, Macdonald ME, Hayden MR, Friedlander RM. Huntingtin inhibits caspase-3 activation. EMBO J. 2006;25:5896-906.

[101] Rigamonti D, Sipione S, Goffredo D, Zuccato C, Fossale E, Cattaneo E. Huntingtin's neuroprotective activity occurs via inhibition of procaspase-9 processing. J Biol Chem. 2001;276:14545-8.

[102] Milnerwood AJ, Cummings DM, Dallerac GM, Brown JY, Vatsavayai SC, Hirst MC, Rezaie P, Murphy KP. Early development of aberrant synaptic plasticity in a mouse model of Huntington's disease. Hum Mol Genet. 2006;15:1690-703.

[103] Bayram-Weston Z, Torres EM, Jones L, Dunnett SB, Brooks SP. Light and electron microscopic characterization of the evolution of cellular pathology in the Hdh((CAG)150) Huntington's disease knock-in mouse. Brain Res Bull. 2012;88:189-98.

[104] Bayram-Weston Z, Jones L, Dunnett SB, Brooks SP. Light and electron microscopic characterization of the evolution of cellular pathology in YAC128 Huntington's disease transgenic mice. Brain Res Bull. 2012;88:137-47.